A microbiosensor for the detection of methane in environmental samples

by

Yijun Chen

A thesis submitted in partial fulfillment of the requirements for the degree of

Master of Science

In

Environmental Science

Department of Civil and Environmental Engineering

University of Alberta

Abstract

The study of methanogenesis in wastewater biofilms and various aggregated methanogenic environmental samples with high spatial resolution can be achieved by using microbiosensor techniques. In this study, the fabrication of a microbiosensor for methane detection was studied. This microbiosensor is composed of an oxygen microsensor, a gas capillary and a media capillary. The methane oxidizing bacteria are immobilized in the media capillary and can consume oxygen from the gas capillary. Associating with the consumption of oxygen, the external partial pressure of methane can be reflected by the signal of the oxygen microsensor. These three components of the methane microbiosensor were assembled together with sensor tip diameter of around 190 μm. The methane microbiosensor can exhibit linear response in the range of 0-1 atm partial pressure of methane when the bacteria have good activity. Alternatively, the methane microbiosensor only exhibits linear response at lower concentrations when the bacteria are less active. To test the performance of the methane microbiosensor, we also applied this technique to the testing of methane concentration in a sludge sample from an anaerobic digester used for municipal wastewater treatment. The results showed that the fabrication and calibration of the methane microbiosensor were successful, and it can be used for measurements of methane concentration in aggregated methanogenic environmental samples.

Acknowledgement

I would like to gratefully and sincerely thank my supervisor Dr. Tong Yu for his guidance, understanding, patience, and encouragement during my graduate studies at University of Alberta. He contributed to a rewarding graduate school experience by giving me intellectual freedom in my work, supporting my attendance at various conferences, engaging me in new ideas, and demanding a high quality of work in all my endeavors.

I'm grateful to Dr. David Zhu and Dr. Aloke Kumar for serving as my committee members, for their encouragement, insightful comments and suggestions. I would also like to thank Dr. Yan Zhang for his assistance and help during my research. We had lots of stimulating discussions, and without his efforts my job would have undoubtedly been more difficult. I am also grateful to Elena Dlusskaya, Chen Liang, David Zhao for helpful suggestions throughout my experiments.

Additionally, my thanks go to my fellow labmates in Environmental Engineering Group: Hong Liu, Miao Yu, Lei Zhu, Zi'ang Zhu. They have provided a friendly and cooperative atmosphere at work and also useful feedback and insightful comments on my work.

Finally, I would like to thank my family. I am very grateful for their support, encouragement, patience and unwavering love. Their faith in me and allowing me to be as ambitious as I wanted have made it possible for me to finish my graduate study in Canada.

Table of Content

List of Figures

List of Tables

List of Abbreviations

CLSM	Confocal Laser Scanning Microscopy
DGGE	Denaturing-Gradient Gel Electrophoresis
DO	Dissolved Oxygen
FISH	Fluorescent In Situ Hybridization
LIX	Liquid Ion-Exchange
MAB	Membrane Aerated Biofilm
MABR	Membrane Aerated Biofilm Reactor
MBBR	Moving Bed Biological Reactor
MMOs	Methane Monooxygenases
NAD	Nicotinamide Adenine Dinucleotide
OD	Optical Density
ORP	Oxidation-Reduction Potential
PCR	Polymerase Chain Reaction
PFGE	Pulse Field Gel Electrophoresis
RBC	Rotating Biological Contactors
SEM	Scanning Electron Microscopy
SRB	Sulfate Reducing Bacteria

1.0 Introduction

1.1 Overview

Together with physical and chemical treatment processes, biological treatment processes play an important part in the wastewater treatment industry. Primarily, biological treatment is used to remove the colloidal or dissolved biodegradable organic substances in wastewater by biological activities (Metcalf & Eddy, 2014). Compared to other types of treatment, it has the advantages of being environmentally friendly and cost-effective. There are two main categories in the biological treatment processes: suspended growth processes and attached growth processes. In suspended growth processes, by mixing, the microorganisms are maintained in liquid suspension in the reactor In the attached growth processes, the microorganisms are attached to an inert media to form biofilm (Metcalf & Eddy, 2014).And the organic material and nutrients flowing past the biofilm are removed from the wastewater by the microorganisms. The attached growth processes are simpler to operate than suspended growth processes. Additionally, they have higher removal rates due to the ability to keep a high loading microorganisms (Loupasaki & Diamadopoulos, 2013). Based on previous research, biofilm is heterogeneous and can be viewed as stratified layers with different microbial activities (Lewandowski & Beyenal, 2013). From the oxic zone to the anaerobic zone inside the biofilm, different microbial metabolisms can happen, including aerobic oxidation, nitrification, denitrification, sulfate reduction,

methanogenesis, etc. The metabolisms can have significant effects on the performance and maintenance of the biofilm reactors. Consequently, the study of these metabolisms inside the wastewater biofilm can provide the theoretical foundation for the design of the biofilm reactors and so as to improve their performance.

A microsensor is a kind of sensor with a tip diameter down to the range of micrometers. It can measure chemical variables with high spatial resolution and is suitable for in situ measurements in the aggregated environmental samples with internal gradients including biofilm, sediments, etc (Lewandowski & Beyenal, 2013). In our laboratory, a series of microsensors were developed, including oxygen, pH, oxidation-reduction potential (ORP), ammonium, nitrite, nitrate, hydrogen sulfide and sulfate microsensors. These microsensors allow us to study four different microbial metabolisms: aerobic oxidation, nitrification, denitrification and sulfate reduction. However, for the study of methanogenesis, there is no available analytical tool.

One kind of microsensor that can provide in situ measurement of methane concentration in aggregated environmental samples was developed by Damgaard and Revsbech (1997). Because it used a kind of bacteria inside the sensor, it is termed a methane microbiosensor. However, because of the complicated fabrication process and relatively short life span, only two laboratories succeeded in developing the sensor (Damgaard & Revsbech, 1997; Satoh et al., 2007) and it is not commercially available so far. To our knowledge, few studies have been done on the methanogenesis inside wastewater biofilms.

Therefore, this study aims to develop a methane microbiosensor that can be applied to in situ measurement of methane concentration in stratified environmental samples, particularly wastewater biofilms.

1.2 Objectives

The overall objective of this study was to develop a functional methane microbiosensor, which includes fabrication, calibration and sample testing.

2.0 Literature Review

This section first briefly introduces the basic concepts of biofilm reactors and the importance of biofilm research on the studies of biofilm reactors. It also discusses the structure of biofilm and microbial activity inside biofilm, with an emphasis on methanogenesis. It summarizes different analytical methods for biofilms characterization, and introduces the concepts of microsensors. Finally, the theory of the methane microbiosensor is introduced.

2.1 Biofilm reactors

Biofilm reactors are used in the attached growth processes. Microorganisms involved in the attached growth wastewater treatment will grow on the surface of the inert media inside the biofilm reactor. The biofilm formed during this process can provide theoretical foundations for the biofilm reactors and have a significant impact on their operations and maintenance (Loupasaki & Diamadopoulos, 2013). Different packing materials can serve as the media for the growth of the microorganisms, including rock, gravel, slag, sand, redwood, and a wide range of plastic and other synthetic materials (Metcalf & Eddy, 2014). Biofilm reactors can be operated as aerobic or anaerobic. The packing can be non-submerged, partially submerged or completely submerged in liquid. (Metcalf & Eddy, 2014). Some examples of common biofilm reactors are tricking filters, rotating biological contactors (RBC), moving bed biofilm reactors (MBBR), etc (Loupasaki & Diamadopoulos, 2013).

2.2 Structure of biofilm and microbial activity inside biofilm

Conventional biofilm has been proved to be heterogeneous by previous research, and two conceptual models about the heterogeneous biofilms have been developed (Lewandowski & Beyenal, 2013). The first model claims that "a biofilm is built with infinite amounts of microcolonies separated by voids filled with water, and the activity of a biofilm is the sum of the activities of the individual microcolonies". Because each microcolony in a biofilm is different and only limited amounts of microbial activity can be measured, it is difficult to study biofilm based on this mode. The second model is the conceptual model of stratified biofilm. Instead of microcolonies, this model views layers as the building block of the biofilm. It assumes that "the heterogeneous biofilm can be subdivided into a finite number of uniform layers and that the activity of the biofilm can be represented by the combined activity of all these layers" (Lewandowski & Beyenal, 2013).

The stratification of biofilm has been demonstrated (Beyenal & Lewandowski, 2005; Yu & Bishop, 1998). Many studies have been done on the microbial activities inside biofilm. Okabe et al. (1999) studied nitrification and denitrification processes in domestic wastewater biofilms. It is found that nitrification happened in the outer part of a biofilm, right below which the denitrification process occurred. Another study on a wastewater biofilm showed that aerobic oxidation took place only in a shallow layer of 0.55 mm near the surface and sulfate reduction occurred in the deeper anoxic zone (Yu & Bishop, 2001). Besides the conventional biofilms, the microbial

metabolisms were also studied in the membrane aerated biofilms (MABs). MAB is a kind of biofilm grown in the membrane aerated biofilm reactors (MABRs). In conventional wastewater bioreactors, oxygen and nutrients are provided from the same direction. However, oxygen is provided to the base of the biofilm and nutrients are provided in the liquid phase above biofilm in an MABR (Lackner et al., 2008). Tan et al. (2013) studied multiple microbial processes inside a piece of MAB including aerobic oxidation, nitrification, denitrification and sulfate reduction. The results showed that both sulfate reduction and denitrification occurred about 550 μm below the interface. About 400 to 450 μm below the interface, the highest H_2S production rates were discovered. High oxygen consumption rates and nitrification occurred at around 750–900 μm and 500–650 μm below the interface, respectively. In another research done by Liu et al. (2014), sulfate reduction and vertical spatial distribution of sulfate reducing bacteria (SRB) in an oxygen-based MAB were studied. The results showed that a high activity of SRB was found in the upper 285 mm of the biofilm. And the maximum SRB biomass was in the upper biofilm. Although it was found that an anaerobic zone was present below the anoxic zone inside the biofilm, the methanogenesis process was not studied.

2.3 Methanogenesis

Methanogenesis, along with aerobic oxidation, nitrification, denitrification, and sulfate reduction, it is one of the major microbial metabolisms existing in the biofilm. It takes place wherever organic matter is decomposed and

external electron acceptors such as oxygen, nitrate or sulfate are depleted (Schink, 1997). The microorganism producing methane in the process of methanogenesis is called methanogen. The microorganism is a type of methane producing archaea, which falls into the group of obligately anaerobic Euryarcheota (Deutzmann et al., 2011). The major substrates that methanogens can utilize are acetate and H_2/CO_2 (or formate) (Zinder, 1993).

Under anaerobic conditions, methanogens and SRB can compete for the same substrates (H_2 and acetate) (Sun et al., 2014). Consequently, sulfate reduction and methanogenesis can coexist in this environment while competing with each other. Raskin et al. (1996) demonstrated that the addition of sulfate into the influent of a fixed-bed biofilm reactor promoted the activity of sulfate reduction and the population of SRB. On the other hand, Methane production and the population of methanogens decreased immediately with the addition of sulfate. The stratified microbial structure and activities of SRB and methanogens in anaerobic sewer biofilms were studied (Sun et al., 2014). It was found that SRB had a higher relative abundance on the surface layer, and methanogens mainly exist in the inner layer of the biofilm.

2.4 Analytical methods for biofilm studies

Biofilm is a complex system of microorganisms surrounded by a matrix of extracellular polymeric substances. The research of biofilms is quite interdisciplinary and it involves scientists from different fields such as microbiology, chemistry, physics and engineering (Denkhaus et al., 2007).

The conventional methods used to analyze biofilm activities are characterization of biofilm mass, biofilm density and total protein (Lazarova & Manem, 1995). However, these techniques can only provide information about biofilm activities at macroscale, which is not sufficient for the biofilm analysis. Many new analytical techniques that can provide information about biofilm activities at microscale have been developed, including microscopy, molecular biology and microsensor techniques.

2.4.1 Microscopic techniques

Scanning electron microscopy (SEM) and confocal laser scanning microscopy (CLSM) are two important microscopy techniques used in biofilm analysis.

As a type of electron microscopy method, SEM can provide a very high image resolution of complex structures (Lazarova & Manem, 1995). Some disadvantages of SEM are complex sample preparation procedures which can cause biofilm shrinkage, damage and biofilm loss. SEM has been widely applied in the research of biofilm. Hawser and Douglas (Hawser & Douglas, 1994) used SEM and reported a model system for studying candida biofilms growth. Yoshida and Kuramitsu (2002) performed SEM analysis of S. mutans biofilms on polystyrene surfaces to study the development of a characteristic three-dimensional biofilm structure. Stenotrophomonas maltophilia biofilms were analyzed by SEM to investigate the correlation between the formation of biofilm on polystyrene and cell surface properties (Pompilio et al., 2008).

CLSM plays an important role in the understanding of many biological processes. It makes it possible to analyze the live, fully hydrated biofilms and can identify different compounds. It allows researchers to get the simultaneous information about the 3-dimensional (3D) structure of the biofilms (Denkhaus et al., 2007). However, it is not suitable for the analysis of very thick and opaque biofilms (Wolf et al., 2002). Auschill et al. (2005) analyzed biofilm samples by CLSM and evaluated the influence of an amine fluoride/stannous fluoride and a chlorhexidine compared with water on in situ biofilm growth. Xavier et al. (2003) developed a software suite of image processing tools that can fully automate biofilm morphology quantification using CLSM images. A 3D model of biofilm detachment is developed based on CLSM data. The results showed that the change of structure during biofilm development plays the key role in the detachment behavior (Böl et al., 2009).

2.4.2 Molecular biology techniques

The development of molecular biology techniques during the 1990s revolutionized the study of microorganisms (Sanz & Köchling, 2007). Unlike traditional methods, it doesn't require the isolation of pure cultures and characterization experiments. Some of the important molecular techniques widely used in the biofilm studies include nucleic acid probes (oligonucleotide probe, DNA microarray) of specific bacterial DNA sequences from target microorganisms, pulse field gel electrophoresis (PFGE), cloning of 16S rDNA, fluorescent in situ hybridization with DNA probes (FISH), denaturing-gradient gel electrophoresis (DGGE) and

polymerase chain reaction (PCR) for amplification of DNA (Denkhaus et al., 2007).

Sanz and Köchling (2007) reviewed molecular biology techniques used in wastewater treatment, with focus on cloning of 16S rDNA, FISH and DGGE. It was summarized that four major steps are involved in the 16S rDNA technology: "(1) the extraction of nucleic acids, (2) amplification of the 16S rRNA genes, (3) sequencing and (4) identification of the isolated clone with the aid of phylogenetic software". Despite lots of time and effort, it can provide precise taxonomical information of the sample. DGGE can give characteristic band patterns for each analyte based on the mobility difference on a gel of denatured DNA-fragments. It is simple and fast, but it cannot provide detailed genetic information of samples. FISH use fluorescent probes to target certain rRNA sequences and can hybridize with them in situ. It can identify, localize and quantify microorganisms. The lack of probes that can hybridize the rRNA sequences is the major limitation of this technique (Sanz & Köchling, 2007).

2.4.3 Microsensor techniques

Microsensors are powerful tools in the biofilm research. Compared with microscopic and molecular biology techniques, microsensor techniques can determine microenvironment conditions and quantify different analytes at the microscale with high spatial resolution and minimum disturbance to samples. Consequently, microsensor technique is an indispensable tool in biofilm research. Two types of microsensors are widely used in biofilm research:

electrochemical microsensors and fiberoptic microsensors. Potentiometric and amperometric microsensors are two types of popular electrochemical microsensors (Lewandowski & Beyenal, 2013).

Fiberoptic microsensors can be used in biofilm research. They can quantify the concentrations of chromophores in a biofilm and in the biofilm microorganisms. With different electronics running the sensor and collecting the data, the optical microsensors can measure either backscattered light intensity or fluorescent light intensity in biofilms (Lewandowski & Beyenal, 2013). Kocincova et al. (2007) developed a type of fiber-optic microsensor that can measure dissolved oxygen (DO), pH and temperature, simultaneously. The tip diameter is around 140 μm and was covered with luminescent microbeads that respond to change in decay time, intensity of their luminescence, or both. Unlike electrochemical microsensors, fiberoptic microsensors are free from the electromagnetic interference, have more geometric versatility, and can stand harsh environments. However, because of the technical difficulties in making fiberoptical microsensors with small tips, their application in biofilm studies is limited (Lewandowski & Beyenal, 2013). Currently, compared to fiberoptical microsensors, electrochemical microsensors are more widely used in biofilm research.

In amperometric microsensors, current is generated as a consequence of oxidation/reduction at the electrode surface when potential is applied to the electrode, and the current is recorded as the analytical signal. In this process, the current is proportional to the concentration of the chemical variables in

the bulk solution (Lewandowski & Beyenal, 2013). Oxygen microsensors and hydrogen sulfide microsensors are two popular types of amperometric microsensors that are used in biofilm research.

Amperometric oxygen microsensor techniques have been among the most reliable and the most mature microsensors in biofilm research. In an oxygen microsensor, oxygen can diffuse through a silicone rubber membrane to the tip of the working electrode. When a negative potential is applied to the cathode, oxygen is reduced to H_2O. At the same time, an oxidation reaction occurs at the anode (Ag/AgCl). Typically –0.8 V is applied as the potential, and the measured current is proportional to the dissolved oxygen concentration at the sensor tip (Lewandowski & Beyenal, 2013). Two types of oxygen microsensors have been developed: separate oxygen microsensor and combined oxygen microsensor. In the separate oxygen microsensor, an external reference anode is placed in proximity to the working cathode. To decrease the electrical interference, the combined oxygen microsensor was developed, which has the working and reference electrodes integrated in one body and the electrolyte inside the body (Lu & Yu (2002). Figure 1 shows a schematic drawing of a combine oxygen microsensor drawn by Lu & Yu (2002).

The first combined hydrogen sulfide microsensor was developed by Jeroschewski et al. (1996). It served as a powerful tool on studies of sulfate reduction and sulfur oxidation in microbial communities. The vertical distribution of SRB was studied by molecular techniques coupled with

different microsensors including hydrogen sulfide microsensor in both aerobic wastewater biofilms and anaerobic sewer biofilms (Okabe et al., 1999; Sun et al., 2014).

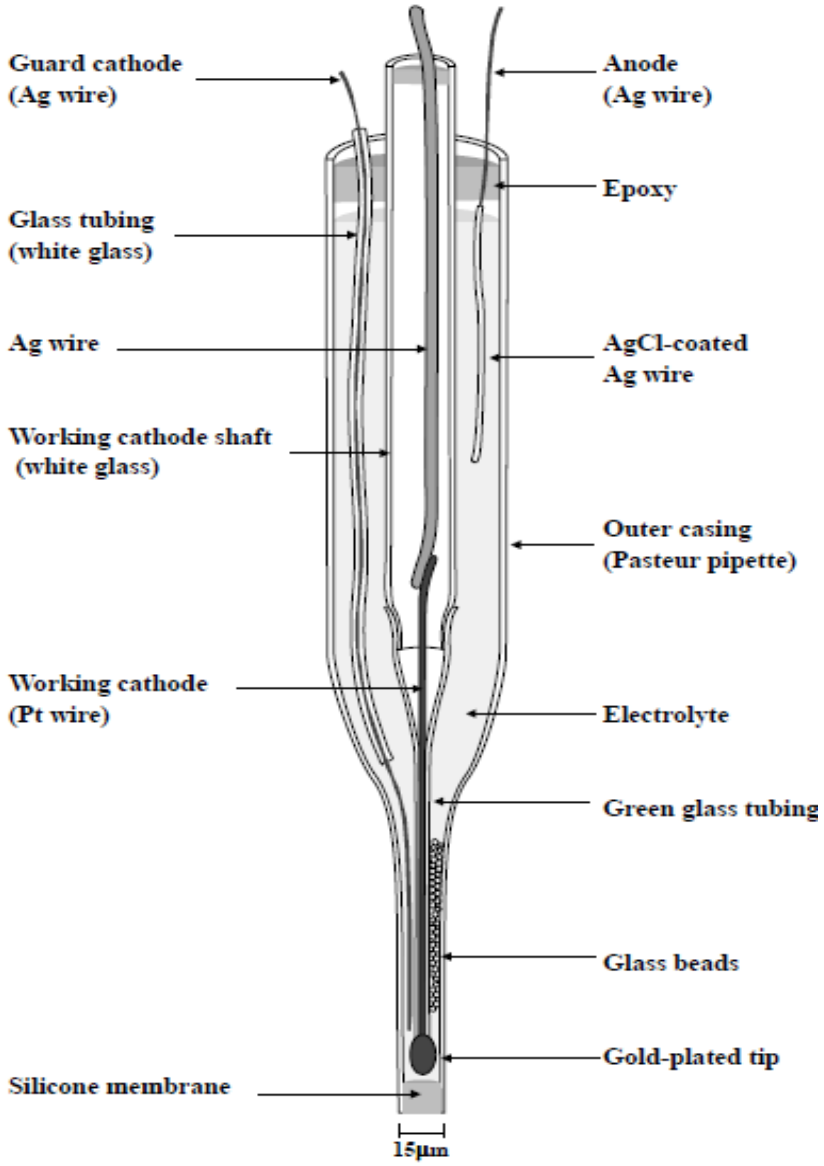

Figure 1 Schematic diagram of the oxygen microsensor (Lu & Yu, 2002).

Microbiosensors are developed based on the theory of amperometric microsensor. The chemical signal that received by the transducer can be modified by the biological compound immobilized on sensing tips. Glucose, methane, nitrate, and nitrous oxide microsensors are examples of successfully miniaturized microbiosensors (Lewandowski & Beyenal, 2013). The theory of the methane microbiosensor will be further discussed in the following section.

Potentiometric microsensors measure membrane potentials. The most popular potentiometric chemical sensors are liquid ion-exchange (LIX) ion-selective microsensors. The potential is proportional to the logarithm of the concentration of analyzed ion. The membrane potential inside a LIX microsensor is shown in Eq. 1(Lewandowski & Beyenal, 2013).

$$E_{cell} = E_{int} - E_{ref} + E_{l-j} + E_{LIX} \quad \text{(Eq. 1)}$$

Where E_{cell} is the cell potential; E_{int} is the potential drop across the internal reference electrode; E_{ref} is potential drop across the external reference electrode; $E_{l\text{-}j}$ is the potential drop across the liquid junction; E_{LIX} is the potential drop across the ion-selective membrane. E_{int} and E_{ref} are known and are fixed to a certain type of sensor (the internal solution in each reference electrode has a fixed composition). For a LIX microsensor, the only variable potential drop is E_{LIX}, which is related to concentration of the analyte (Lewandowski & Beyenal, 2013). Although LIX microsensors have a longer equilibrium time and shorter life span compared to amperometric microsensors, they are easier to fabricate.

Potentiometric microsensors have been developed to measure pH, ammonium, nitrate, nitrite and sulfide. pH, ORP, ammonium microsensors were used to study the redox potential changes in both aerobic/sulfate-reducing biofilm and aerobic/nitrification biofilm (Yu & Bishop, 1998). Satoh et al. (2012) studied microbial community structures and their activities in single anaerobic granules by the use of pH, ORP and other microsensors, coupled with molecular techniques.

2.5 Theory of the methane microbiosensor

This section briefly explains the basic theory of the methane microsensor, more detailed information about the functioning of the methane microbiosensor will be explained in section 4.1. The basic theory of methane microbiosensor is based on the methane microbiosensor developed by Damgaard and Revsbech (1997). The methane microbiosensor is composed of three parts: an oxygen microsensor and two layers of gas capillaries outside the oxygen microsensor, which are termed gas capillary and media capillary (Figure 2). The tips of the three parts are all sealed with silicone membrane. The silicone membrane is a kind of silicone rubber and the basic structure is shown in Figure 3. The siloxane bond (Si-O-Si) forms the basic helical structure, and outside the structure are the methly groups which can rotate freely. Because of the structure, the silicone membrane is water resistant and permeable to gas molecules (Characteristic properties of Silicone Rubber Compounds, 2012).

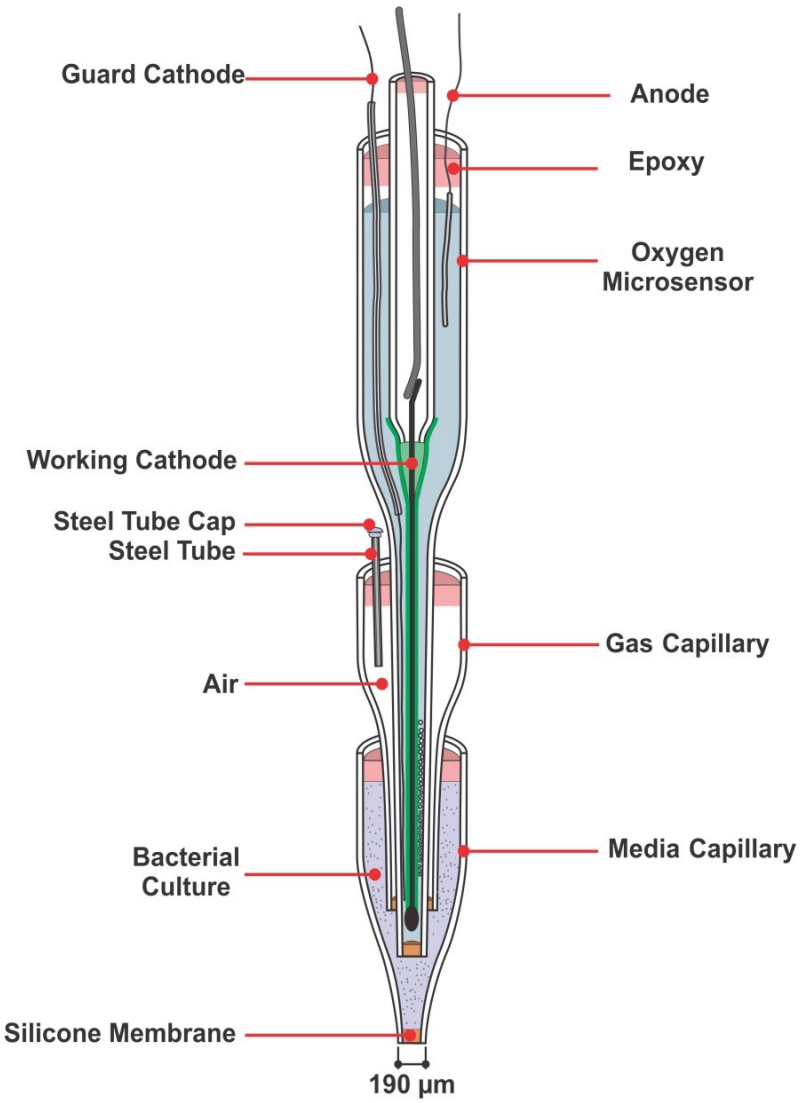

Figure 2 Schematic diagram of the methane microbiosensor

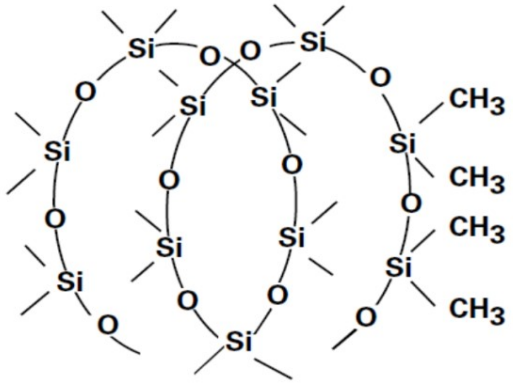

Figure 3 The basic structure of silicone rubber (Characteristic properties of Silicone Rubber Compounds, 2012)

As it is shown in Figure 2, the oxygen microsensor and one steel tube are inserted into the gas capillary. The shaft end of the gas capillary and the steel tube was fixed to the shaft end of the oxygen microsensor with epoxy. Likely, the combined oxygen microsensor and gas capillary is inserted into the media capillary and sealed with epoxy at the shaft ends. The space between the oxygen microsensor and the gas capillary is filled with atmospheric air. And this space is termed gas space. A small piece of glass tube sealed with dental wax serves as the cap of the steel tube. The steel tube can be used to change the air inside the gas space. The space between the gas capillary and media capillary is termed reaction space. And it is filled with a culture of *Methylosinus trichosporium* OB3b. This is a kind of methane oxidizing bacteria. This kind of bacteria can generate the enzyme methane monooxygenases (MMOs). There are two forms of MMOs: a soluble,

cytoplasmic enzyme complex (sMMO) and a membrane bound, particulate enzyme system (pMMO) (Xin et al., 2002). Researchers have found that sMMO is present only when the concentration of cooper is low, and pMMO predominates when the cooper concentration is high (Takeguchi et al., 1998). Scott et al. (1981) also proved that the gas mixture used to cultivate the bacteria could also affect the activity of pMMO and sMMO. In their research, it was found that bacteria grown in 15:1 (vol/vol) methane/oxygen mixture had around 30%-66% pMMO activity out of all the MMO activity. The activity of sMMO predominates when the bacteria were grown in 1:5 (vol/vol) methane/oxygen mixture. And the concentration of $CuCl_2 \cdot 2H_2O$ used in the medium was 2.5 μg/L.

The tip of the methane microbiosensor is shown in Figure 4. Methane can diffuse into the reaction space from the tip of the sensor and oxygen can diffuse from the gas space. The reaction is described by Eq. 2.

$$CH_4 + O_2 + NADH + H^+ \xrightarrow{MMOs} CH_3OH + NAD^+ + H_2O \quad \text{(Eq. 2)}$$

In this equation, NADH and NAD^+ are the reduced and oxidized forms of nicotinamide adenine dinucleotide (NAD), respectively.

Consequently, any change of the concentration of the methane will result in the change of the concentration of oxygen, which can be reflected by the signal of the oxygen microsensor.

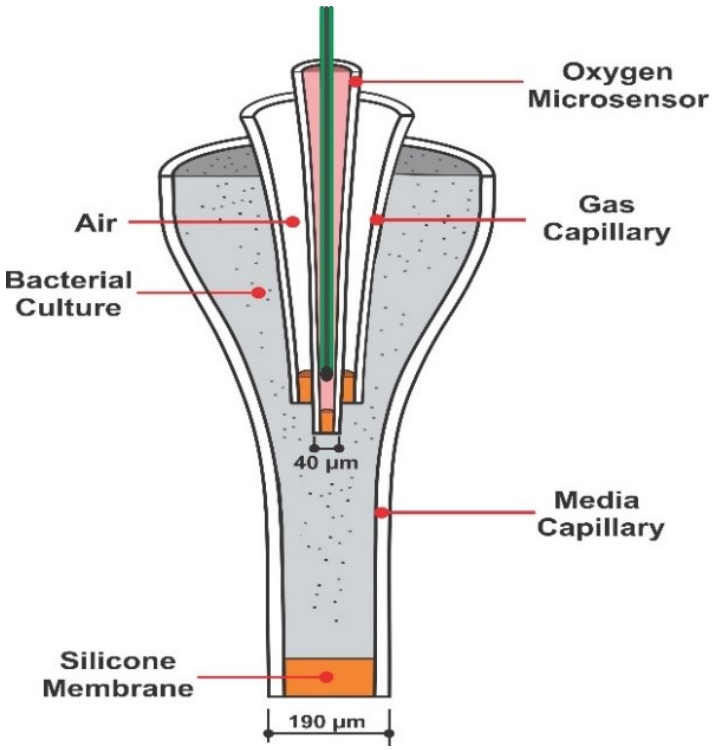

Figure 4 Schematic diagram of the tip of the methane microbiosensor

3.0 Fabrication of the methane microbiosensor

This section explains how a methane microbiosensor is fabricated. The processes include: bacteria cultivation, fabrication and calibration of the oxygen microsensor, fabrication of the gas and media capillaries, assembling gas capillary, assembling the media capillary and injecting the bacteria.

3.1 Bacteria cultivation

Biosensors use biological material to modify chemical signal received by the transducer (Lewandowski & Beyenal, 2013). In methane microbiosensors, *Methylosinus trichosporium* OB3b is used to modify the signal of the sensor. This kind of bacteria can use methane as sole source of carbon and energy, and it is a type of methanotrophic bacteria (methanotrophs). Previous studies have revealed that only a few of the methanotrophs that are present in the environment have been successfully isolated and cultured in laboratory, and *Methylosinus trichosporium* OB3b is one of the best characterized methanotrophs among them (Murrell, 2010).

3.1.1 Bacteria cultivation methods

The culture of *Methylosinus trichosporium* OB3b was purchased from the American Type Culture Collection (ATCC 49243). An ammonium mineral salts medium as described in Table 1 was used to cultivate the bacteria.

Table 1 The composition of ammonium mineral salts medium

Substance	Amount
K_2HPO_4	0.7 g/L
KH_2PO_4	0.54 g/L
$MgSO_4 \cdot 7H_2O$	1.0 g/L
$CaCl_2$	0.2 g/L
$FeSO_4 \cdot 7H_2O$	4.0 mg/L
NH_4Cl	0.5 g/L
$ZnSO_4 \cdot 7H_2O$	100.0 μg/L
$MnCl_2 \cdot 4H_2O$	30.0 μg/L
H_3BO_3	300.0 μg/L
$CoCl_2 \bullet 6H_2O$	200.0 μg/L
$CuCl_2 \cdot 2H_2O$	10.0 μg/L
$NiCl_2 \cdot 6H_2O$	20.0 μg/L
$Na_2MoO_4 \cdot 2H_2O$	60 μg/L
Agar (For slant test only)	15g/L

Appropriate amounts of nutrients except KH_2SO_4, K_2HSO_4 and $FeSO_4$ were added to distilled water and sterilized by autoclaving. Because Mg^{2+} and PO_4^{3-} can form insoluble $Mg_3(PO_4)_2$ at high temperatures, appropriate aliquots of concentrated solutions of KH_2SO_4 and K_2HSO_4 were sterilized through a 0.22 μm membrane filter (Merck Millipore Ltd., (Fisher Scientific Cat. #.: SLGV033RS)) and added to the rest of the sterilized medium solution. Concentrated $FeSO_4$ solution was sterilized through the 0.22 μm membrane filter, and added in the same way due to its instability at high temperature.

The culture was first cultivated on slants and then in flasks under 1:1 (vol/vol) methane/air mixture (corresponding to 5:1 methane/oxygen). As it was mentioned in section 2.5, both cooper concentration and gas mixture used during the cultivation can affect the activity of pMMO and sMMO. Compared to the experiments done by Scott et al. (1981), the methane to oxygen volume ratio falls into the middle of the ranges of 15:1 to 1:5. Additionally, the medium used in this research had a high $CuCl_2 \cdot 2H_2O$ concentration (10 µg/L compared to 2.5 µg/L). Consequently, it was very possible that pMMO would contribute a significant part of the total MMO activity.

To transfer the freeze dried culture purchased from ATCC to the slants, 0.5 mL medium was first added to the culture to rehydrate the entire pellet. This aliquot was then transferred into a sterilized tube with 1.5 ml medium in it. The culture was mixed well with the medium in the tube. 0.1 ml of the culture was transferred to each slant. The slants were incubated in a closed chamber (Becton Dickinson Inc., Canada （Fisher Scientific Cat.#: B26062)). The chamber was first partially evacuated with a portable vacuum pump (Cat. #.: S90724A, Fisher Science Education, Canada) which had a meter on it, and then filled with methane from a balloon to give a mixture of methane and air (1:1, vol/vol) at atmospheric pressure. The chamber was then put in the incubator (Cat. #.: 11675209, Fisher Scientific, Canada) which operated at 25 ℃, and the gas inside the chamber was replaced every 24 h. According to the manual provided by ATCC, *Methylosinus trichosporium* OB3b should be

cultivated for 5-7 days. Based on the experimental observation, the concentration of the bacterial culture increased between day 5 and day 7. Consequently, 7 days were chosen for both the slants and flasks experiments. Some more experiments were done to confirm the optimal time for the bacteria cultivation (will be discussed later).

After 7 days, the culture was transferred to the flasks to cultivate. Flask experiments were performed in 300 mL Erlenmeyer flasks. After inoculation, flasks were sealed with rubber stoppers which had a hole on each of them. A 4-cm-long glass tubing was inserted into each of the holes. One rubber tubing was connected onto the glass tubing which could be sealed with a clipper. The flasks were partially evacuated with a portable vacuum pump to give an inner pressure of 380 mmHg. Methane was added with a 150 mL syringe to give a 1:1 (vol/vol) methane/air mixture inside the flasks. Finally, the rubber tubing was sealed with the clipper. The flask experiments were performed at 25 ℃ in the incubator at the speed of 250 rpm. The gas inside the flasks was replaced every 24 h. The bacteria were cultivated for 7 days in the flasks. The cells were then harvest by centrifuging at 7400 × g for 15min. And the pellet was stored in 15 ml centrifuge tube with 2 mL medium in it at 4 ℃ before use.

To confirm the optical growth time for the bacteria and improve the bacterial growth for future studies, cell density was monitored. Monitoring of the cell density was done in the 25 ml glass tube. Bacteria were inoculated into the glass tubes containing around 10 ml liquid medium. The tubes were closed

with caps which allow air exchange. Then they were fixed in the closed chamber filled with 1:1 (vol/vol) methane/air mixture. The chamber was fixed on the shaking plate of the incubator with an adhesive mat (Infors-Ht, Switzerland (Rose Scientific Cat. #: 63240).

Originally, 25 ℃ was used for the cultivation based on the manual provided by ATCC. However, it was found that the specific growth rate was higher at 30 ℃ than it was at 25 ℃ for this kind of bacteria (Park et al., 1991). To increase the bacteria amount that can be gained from each cultivation, the temperature was increased to 30 ℃ when monitoring the cell density. Additionally, to increase the gas exchange with the liquid medium, the speed of the shaking plate was increased to 300 rpm. The cell density was monitored with a spectrometer (Novaspec II, Pharmacia Biotech) at 600 nm every 24 h for ten days.

The most crucial thing during the bacteria cultivation was to make sure there was no contamination. The contamination from other microorganisms could potentially affect the activity of *Methylosinus trichosporium* OB3b and consequently affect the signal of the sensor.

3.1.2 Bacteria cultivation results

Optical density can be used as a tool to monitor the concentration of bacteria. OD of the bacteria was monitored in three separate glass tubes. To determine when the bacteria reach the maximum optical density, the OD of each of the tubes was monitored for 10 days. The average of three measurements was

used to generate the results, and the error bars represent the standard deviations of triple measurements (Figure 5). It was shown that the value of OD reached its maximum on the seventh day. Although the concentration had a peak between day 2 and day 3, it is not considered as this is not in the range of time that ATCC recommends. Consequently, it was confirmed that bacteria should be collected 7 days after the start of the cultivation. Because the bacteria that were used in the sensor were cultivated at 25 ℃ in the incubator with the speed of 250 rpm, whether or not the change of the cultivation condition (30 ℃ in the incubator with the speed of 300 rpm) will affect the performance of the methane microbiosensor should be further studied.

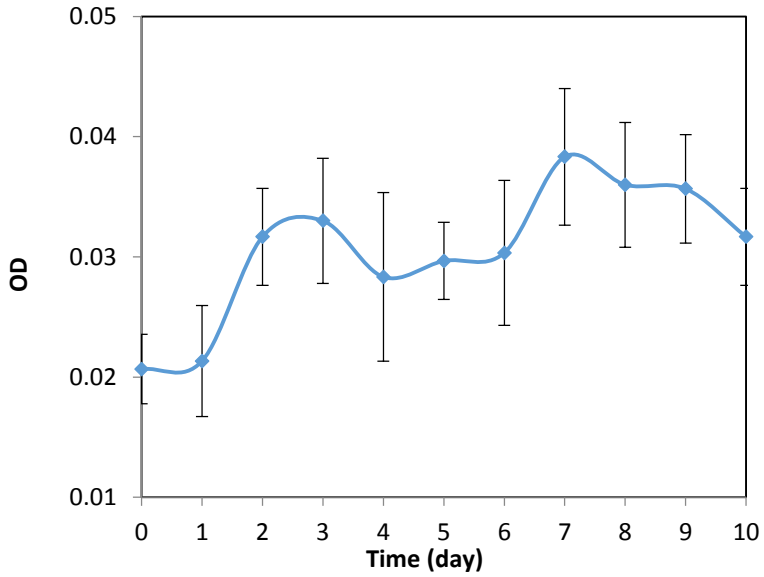

Figure 5 Bacteria growth curve for 10 days

3.2 Fabrication and calibration of the oxygen microsensor

Oxygen microsensor is the core of the methane microbiosensor. It works as a transducer to monitor the concentration of oxygen in the reaction space, which in turn reflects the concentration of methane. As another two layers of glass capillaries were to be assembled outside the oxygen microsensor, it was very crucial to make the oxygen microsensor to the right shape and size. One of the most challenging parts during the fabrication process was to explore the right geometries for the three major parts of the sensor: oxygen microsensor, gas capillary and media capillary. Additionally, it was equally important to fabricate them to the right geometries so that they could fit and being assembled together.

The fabrication approach of the oxygen microsensor is based on the procedures described by (Lu & Yu, 2002). The length of the oxygen microsensor was around 13 cm. The diameter was around 30 μm to 40 μm at the tip and not exceeding 50 μm for several hundred micrometers from the tip.

The polarization and calibration for the oxygen microsensor were conducted by connecting the sensor to a picoammeter (Model: PA2000, Unisense, Denmark). The polarization voltage is −0.80 V. The calibration was conducted by two points: nitrogen gas (0% oxygen) and compressed air (21% oxygen, DO 8.7 mg/L).

3.3 Fabrication of the gas and media capillaries

The gas and media capillaries are the two extra glass layers outside the oxygen microsensor. They serve as the oxygen and bacterial culture reservoir, respectively. The key of the fabrication was to precisely control the shape and size of them, especially for the gas capillary. This is because it is in the middle between the oxygen microsensor and the media capillary, and not having the right geometry will lead to the failure of assembling the three parts together. The detailed information about the dimensions of different parts of the methane microbiosensor is summarized in Table 2.

During the fabrication process, the fine section of a cleaned Pasteur pipette (Cat. #.: 13-678-20C, Fisher Scientific, Canada) was first heated over the natural gas burner and then pulled until an inner diameter of around 0.5mm was obtained. The exact heated location was 11.5 cm from the shaft end of the pipette for the gas capillary and 10.5 cm for the media capillary. About 7 cm of un-pulled end was cut away for the gas capillary and 8.5 cm for the media capillary.

The setup for tapering the gas and media capillaries is shown in Figure 6. It was composed of a micromanipulator, an omega-shaped heating loop that was connected to a porcelain socket, an extension clamp stand, a power control, a foot switch, a microscope, a beaker and a light source. The fine end of the capillary was clipped with a rod which was connected to the micromanipulator (Model: M3301R, World Precision Instruments Inc., USA). In this process, the pulled section of the pipette was placed in the omega-

shaped heating loop with the heated point located at about 12.5 cm from the shaft end for gas capillary and 12 cm for media capillary. The movement of the capillaries was viewed through the horizontal dissection microscope (Model: Stemi SV11, Carl Zeiss, Jena, Germany). By gradually turning up the power supply, the glass started melting and gradually dropping down. At the same time the pipette was slowly moving downward by the control of the micromanipulator. The voltage is doubled by the control of a foot switch until a certain length of new pulled glass capillary was formed (around 3.5 mm for gas capillary and 2 mm for media capillary). Finally, the whole pipette shaft dropped into the beaker underneath which had napkins on its bottom. The capillary tip end was then cut by a microdissecting tweezer (Cat. #: RS-4905, Roboz Surgical Instrument Co., USA) under a vertical microscope with a built-in scale (Model: Axioskop 2 Plus, Carl Zeiss). And the final diameter of the tip was between 60 μm to 90 μm for the gas capillary and between 110 μm to190 μm for the media capillary. Both the gas and media capillary were stored in a container and fixed with putty clay (Van Aken International Rancho Cucamonga, CA, USA).

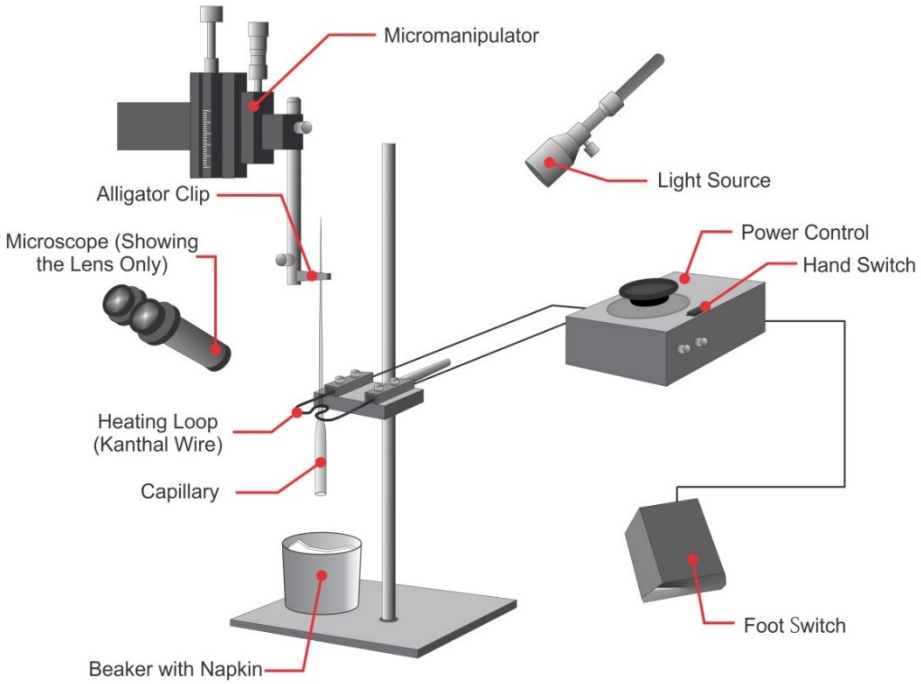

Figure 6 Schematic diagram for tapering of gas and media capillary

3.4 Assembling the gas capillary

As it is shown in Figure 2, in methane microbiosensors, the first layer outside the oxygen microsensor is the gas capillary. Assembling the gas capillary onto the oxygen microsensor should be done very carefully, because both the gas capillary and the oxygen microsensor are easily broken when trying to assemble them together.

The gas capillary was horizontally fixed by the clay on the vertical microscope stage. The oxygen microsensor was gently inserted from the shaft end into the gas capillary. The tip of the oxygen microsensor protrude slightly through the tip of the gas capillary. Then a steel tube with an inner diameter of 0.5 mm (Cat. #: BK18R ,K-Tube Corporation, Poway, CA, USA) was inserted to the shaft end of the gas capillary. The end of the steel tube which is outside the gas capillary is called the access end. One small glass tube sealed with dental wax (Cat. #.: 00403, Polysciences, Inc., Warrington, PA, USA), which served as the cap of the steel tube, was glued on the access end of the steel tube. Some epoxy (Conglom Inc., St. Laurent, QC, Canada) was applied at the shaft end of the gas capillary to fix the oxygen microsensor and the steel tube to the gas capillary as well as to seal off the gas phase. A Pasteur pipette covered with silicone (Cat. #: 31003, Marineland, Blacksburg, VA,USA) at its tip was then horizontally mounted on a micromanipulator and brought in contact with the tip of the gas capillary to give an approximately 60-µm-thick silicone membrane at the tip of the gas capillary.

3.5 Assembling the media capillary and injection of the bacteria

The media capillary is the last layer of glass that is outside the oxygen microsensor. The key of this step is to properly add the bacterial culture to the media capillary, especially to make sure there is no gas bubble at the tip.

The media capillary was first sealed with an approximately 100-μm-thick silicone membrane by a horizontally mounted Pasteur pipette. And it was allowed to dry overnight before any liquid was added into the media capillary. Around 5 μL of sterilized distilled water was added right to the tip of the gas capillary by a 1 mL syringe (Cat.# 309597, Becton Dickinson & Co., USA) of which the tip was heated and pulled to a capillary. If there was any gas bubbles at the tip, some more sterilized distilled water was injected to the tip by the syringe to push the bubble out from the tip.

Bacteria were harvested from 3 flasks during each 7 day experiment by centrifugation (7400 × g for 15min). The resulting pellets were stored in the 15 ml centrifuge tube with 2 mL medium in it at 4 ℃ before use. Before injecting the bacteria into the sensor, the stored pellets were taken out from the fridge. The pellets collected from 12 flasks were transferred to a 15 ml tube and mixed with 10 ml of medium. The tube was closed with a cap which allowed air exchange. Then the tube was fixed in the closed chamber filled with 1:1 (vol/vol) methane/air mixture. The chamber was fixed on the shaking plate of the incubator with an adhesive mat (Infors-Ht, Switzerland (Rose Scientific Cat. #: 63240)). The bacteria were cultivated in the incubator at

25 ℃ for 24h with the speed of 250 rpm. This process would allow the bacteria to regain its activity before being injected into the sensor.

After 24h, the bacteria were collected by centrifugation (7400 × g for 15min). A few hundred microliters of medium was added to the resulting pellet. The pellet was mixed with the media until the bacteria was evenly distributed in the medium. Around 10 μL of the bacterial culture was added to the media capillary to mix with the distilled water. Then the media capillary was horizontally fixed by the putty clay on the microscope stage of a vertical microscope, and the gas capillary with oxygen microsensor inside was gently inserted from the shaft end into the media capillary. The distance between the tip of the oxygen microsensor and the media capillary was between 150 μm to 420 μm. Epoxy was then applied to glue the gas capillary to the media capillary, but an open space between them was still kept for future addition of medium. The epoxy was allowed to dry for 1 hour at room temperature before some more medium was added to the media capillary until it was full of liquid. Finally, some more epoxy was applied to seal the reaction space (definition see page 17). The fabrication of the methane microbiosensor was completed after the epoxy was allowed to dry for 1 hour at room temperature. The methane microbiosensor was fixed with a one-hole rubber cork and inserted into a test tube. To keep the activity of the bacteria, the tube was stored in a 4℃ refrigerator.

4.0 Functioning and evaluation of the methane microbiosensor

This section discusses the fundamentals about functioning of the methane microbiosensor followed by the evaluation of the methane microbiosensor. The major purpose of the evaluation of the methane microbiosensor are: (1) to verify that the fabrication of methane microbiosensor is effective and every step has been carried out correctly, (2) to obtain the calibration curve that can be used for sample measurements, (3) to demonstrate that the methane microbiosensor can be used for the measurement of methane in environmental sample. To achieve these purposes, the calibration of the methane microbiosensor was performed. In this study, two methane microbiosensors (methane microbiosensor 1 and methane microbiosensor 2) were successfully fabricated and calibrated. Additionally, one methane microbiosensor (methane microbiosensor 1) was also applied to test the methane concentration in a sludge sample from an anaerobic digester used for wastewater treatment.

4.1 Functioning of the methane microbiosensor

Methane microbiosensors function based on the theory that the methane-oxidizing bacteria consume oxygen when the tip of the sensor is exposed to methane. The change of the oxygen concentration in the reaction space can be reflected by the signal of the oxygen microsensor inside the sensor.

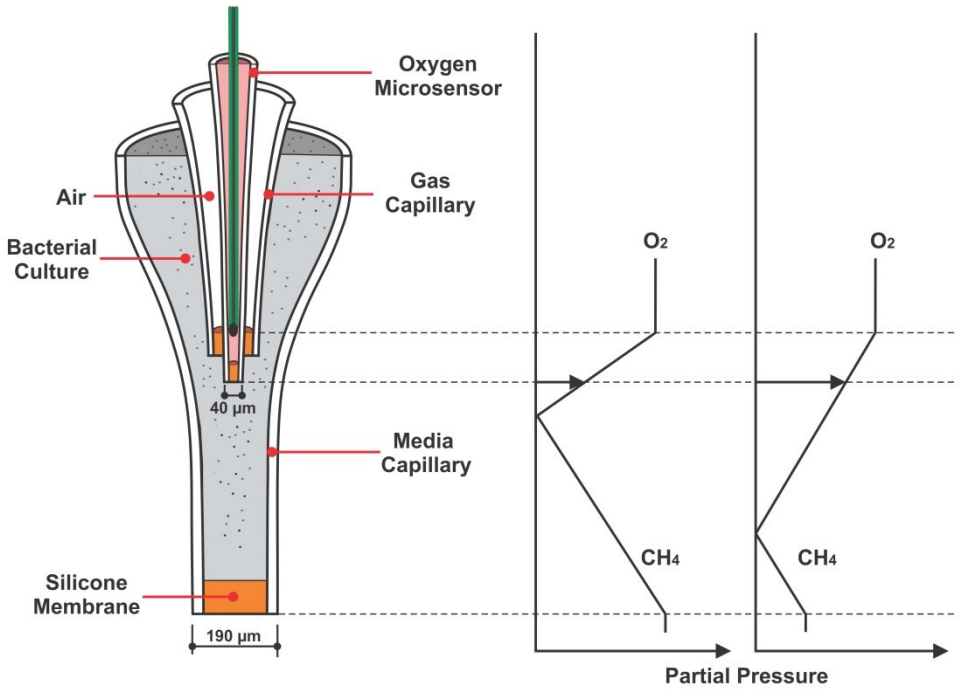

Figure 7 Schematic model of the gradients of oxygen and methane

Figure 7 shows a simplified model of the partial pressure profiles of oxygen and methane inside the sensor. The top dotted line marks the location of the top side of the gas capillary membrane. The middle dotted line marks the oxygen microsensor tip, and the bottom one marks the methane microbiosensor tip. The arrows show the signal of the methane microbiosensor. It can be seen that the higher the partial pressure of methane at the sensor tip is, the more oxygen it can consume in the reaction space, and consequently lower the signal of the sensor will be. Reversely, the lower the methane partial pressure is, the higher the signal will be. This model assumes that the diffusivities in the silicone membrane and media are the same for both oxygen and methane. Additionally, this model is only valid when the

capacity of the bacteria to consume oxygen and methane is not exceeded. Because the silicone membrane is permeable to gas, any oxygen diffusing from the sensor tip into the reaction space can increase the signal of the oxygen microsensor inside. Consequently, oxygen is the major gas that interferes the signal, and methane microbiosensor is most suitable for measurements in anaerobic environments. Besides methane and oxygen, some other common gas that can diffuse into the methane microsensors are: H_2S, CO_2, N_2 and H_2. It was found that when the concentration of H_2S is above 100 μM, it could decrease the signal of the methane microbiosensor. And CO_2 could increase the signal when the oxygen microsensor inside the methane microbiosensor was extremely slim (Damggard & Revesbech, 1997). No interference of signal was found from N_2. Whether or not H_2 can interfere the signal was not studied. However, because H_2 is one of the substrates for methanogens, it is likely to be consumed up in the methanogenic environment and not to exist in significant amount in reaction space of methane microbiosensor.

Many factors can influence the signal of the methane microbiosensor. The characteristic of the oxygen microsensor is the major factor that determines the signal of the methane microbiosensor. It is mainly affected by the cathode area of the oxygen microsensor which is unique for every different oxygen microsensor. Larger cathode area tends to have higher signal. Apart from that, the activity of the bacteria can also influence the signal. The more active the bacteria are, the more capacity they have to consume oxygen, and

consequently the larger the working range of the sensor will be. Damggard and Revesbech (1997) also found that the distance between the oxygen microsensor tip and the gas capillary tip can influence the signal.

4.2 Calibration of the methane microbiosensor

Because each methane microbiosensor is uniquely fabricated and has different configuration, each one of them needs to be calibrated before being used for measurements.

Calibration can be done by two different methods. In the first method, the methane microbiosensor can be exposed to different partial pressures of CH_4 and the signal of the sensor was recorded. Specifically, the methane microbiosensor can be placed in the synthetic medium in a calibration chamber. CH_4 and N_2 are blown into the chamber at different rates. The signal of the sensor was recorded after stabilization. And the headspace method (Bandara et al., 2011), which serves as one of the steps in this first method, can be used to calculate the dissolved methane concentration (Satoh et al., 2007). This method can provide very precise concentrations of methane but the calibration process is relatively complicated and time consuming. Alternatively, the second method which was used in this study uses a specially designed device to perform the calibration process. This method can provide sufficient amounts of data points on the calibration curve with small efforts (Damgaard & Revsbech, 1997).

4.2.1 Calibration method

The calibration setup is shown in Figure 8. Calibration process was carried in a specially designed calibration device which contains two cylindrical chambers. The two chambers were separated by a 5-mm-thick Plexiglas disk with one hole in the middle. The hole was 3 mm wide and filled with agar. The lower chamber has two openings, one for the inlet of the gas, and the other for the outlet of the gas. The upper chamber can be closed with a Plexiglas disk which has a hole in the center. The upper chamber has one opening for the inlet of the gas. Humidified methane gas and nitrogen gas was continuously flushed into the lower chamber and upper chamber respectively for at least 1.5 hours, allowing a linear concentration gradient of methane established through the agar plug.

One methane microbiosensor was mounted on a micromanipulator and connected to the picoammeter. It was then inserted through the hole of the Plexiglas disk while both methane and nitrogen gas was kept flushing. The tip of the methane microsensor was stepwise advanced into the agar by the movement of the micromanipulator. The signal at different locations within the agar was recorded. And the calibration was performed in a Faraday cage (Technical Manufaturing Corporation, USA) to reduce potential electric interference.

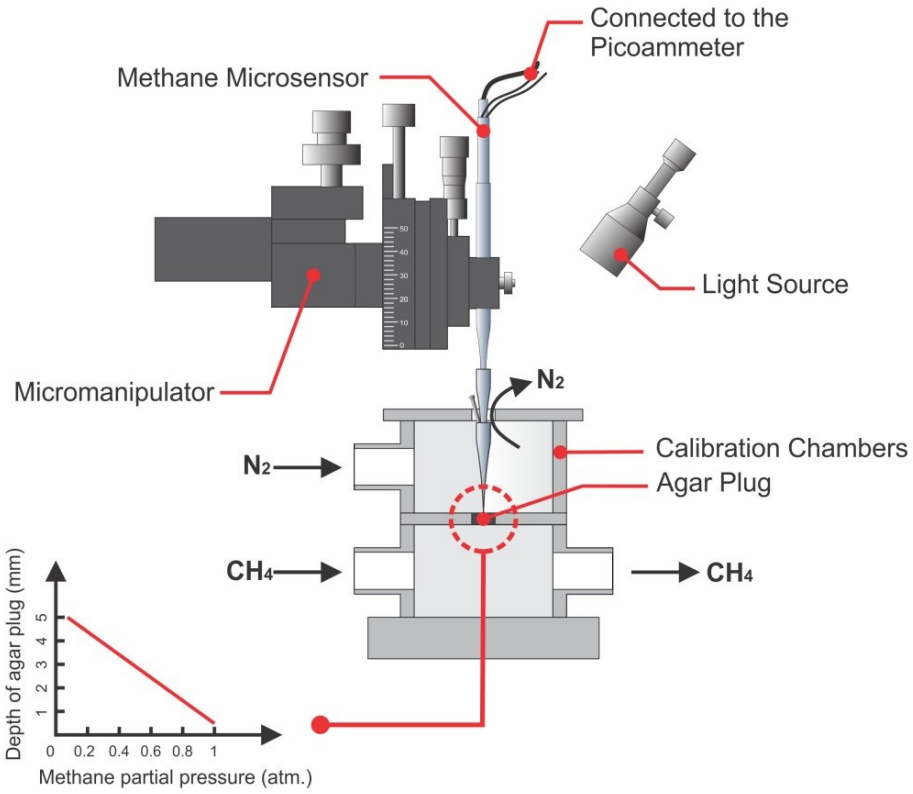

Figure 8 Experimental setup for calibration

To ensure the gas capillary was of 100% atmospheric air, the gas inside the gas capillary was replaced with fresh air before the measurement for calibrations that were done 24h after the fabrication. This was done by firstly melting the dental wax with a flame. After the wax was melted , the air inside the gas capillary was sucked out by using a 1 mL syringe (Cat.# 309597, Becton Dickinson & Co., USA) of which the tip was heated and pulled to a capillary. In this way, Fresh air would refill the gas capillary automatically.

4.2.2 Calibration results

The signal of the methane microbiosensor was recorded for 100 s at each location. The signal stayed relatively stable within 100s. This relatively quick response time agrees with the assumption that the pMMO were present in the bacteria. Methane and oxygen can be readily consumed once they reach the bacteria cell membrane. The average value of the last ten stable signals of the sensor was used to generate the calibration curve. The error bars represent the standard deviation of the 10 measurements.

The calibration curves for 2 different methane microbiosensors (methane microbiosensor 1 and methane microbiosensor 2) are shown in Figure 9, Figure 10 and Figure 11. For methane microbiosensor 1, it was calibrated on both day 2 and day 6 after the completion of fabrication. The calibration curves are shown in Figure 9 and Figure 10, respectively. And microsensor 2 was calibrated on day 5 after the completion of fabrication (Figure 11).

From Figure 9, it can be seen that methane microbiosensor 1 displayed linear response towards methane partial pressure on day 2 between 0 to 1 atm, which covers the range of methane concentration for most environmental samples. It also has a long signal range (around 90 pA). This calibration curve contains sufficient amounts of data points (27 points) and has a good R^2 (0.983). Consequently, it is demonstrated that this fabrication and calibration process is successful.

Microsensor 1 and microsensor 2 displayed linear response only at lower partial pressure of methane on day 6 and day 5, respectively (Figure 10 and

Figure11). This may due to the decrease of the bacterial activity and the capacity of the bacteria was exceeded at higher concentration. Although methane microbiosensors that have this type of calibration curve cannot be used for samples with relatively high concentrations of methane, they have higher sensitivity at low concentrations.

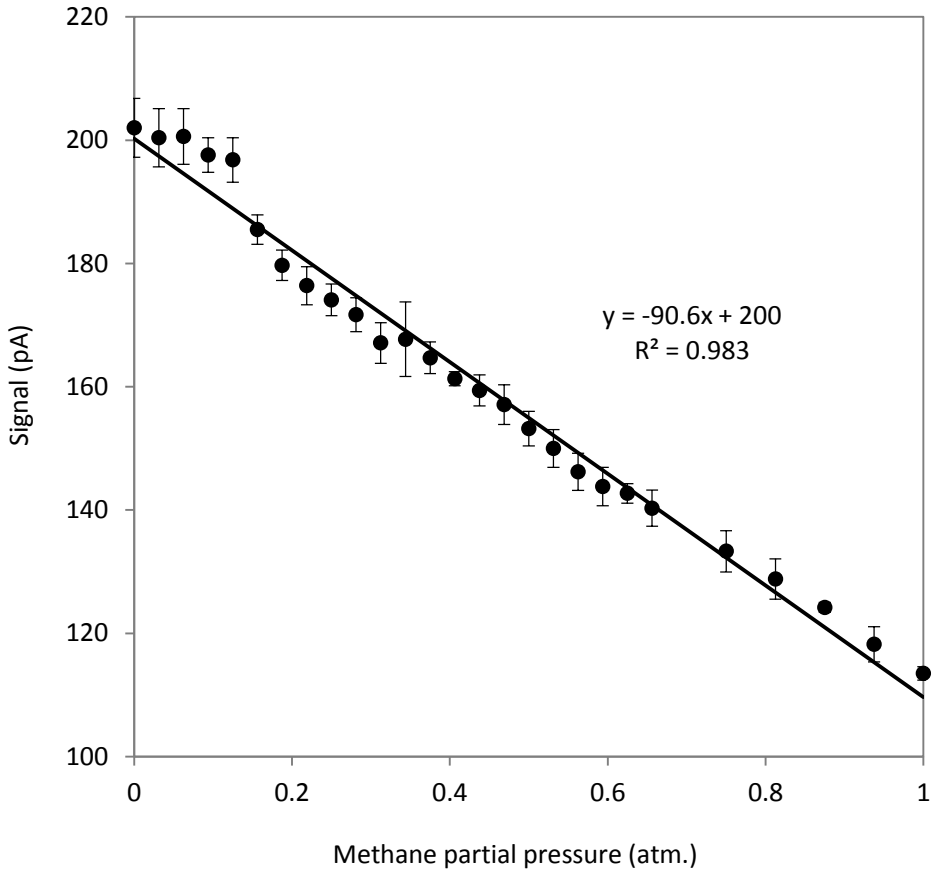

Figure 9 Calibration curve for methane microbiosensor 1 on day 2

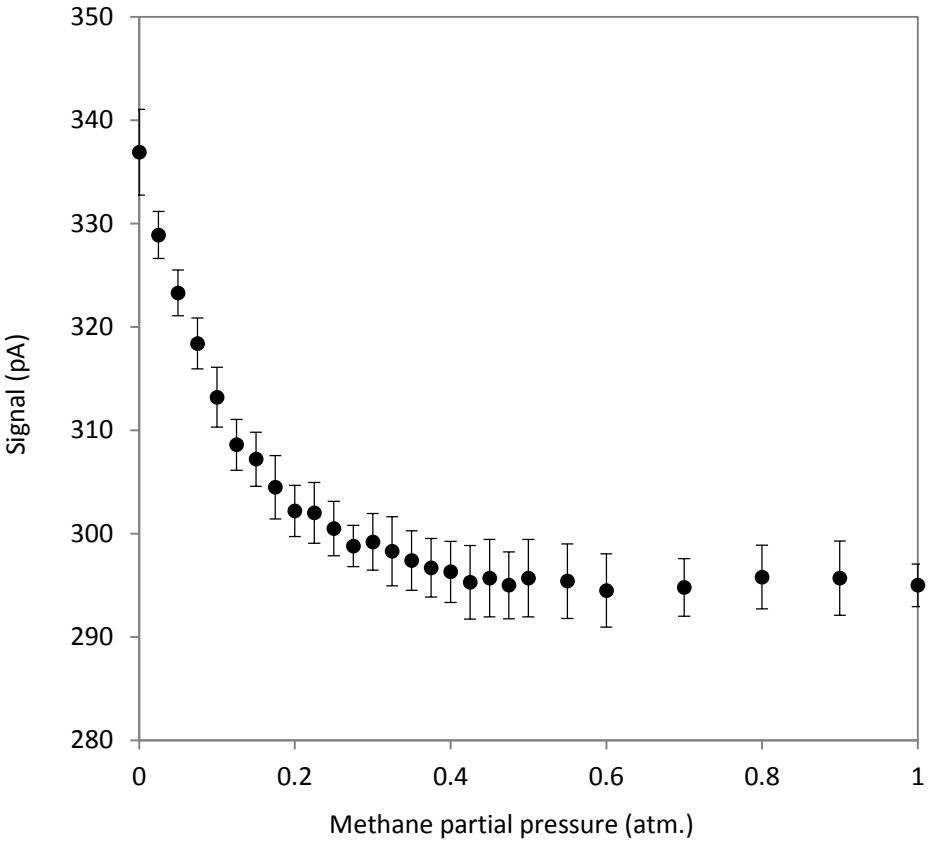

Figure 10 Calibration curve for methane microbiosensor 1 on day 6

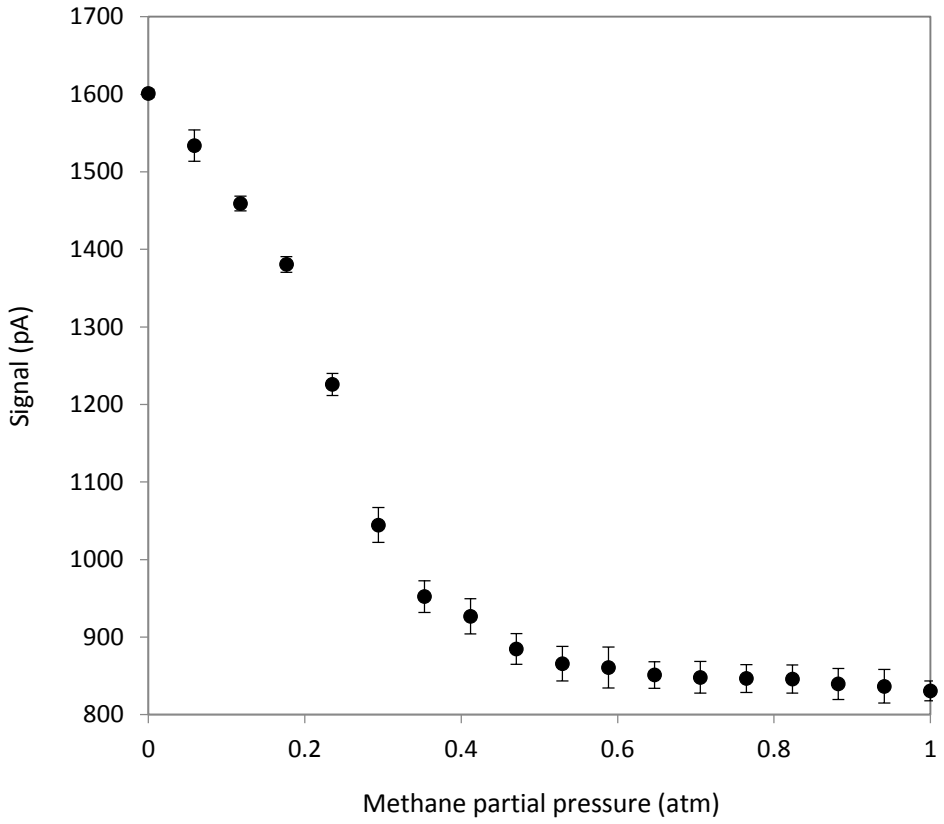

Figure 11 Calibration curve for methane microbiosensor 2 on day 5

Figure 12 shows the calibration curves for methane microbiosensor acquired by Damgaard and Revsbech (1997). As can be seen from Figure 12A, the sensor exhibited a linear response in whole range of 0-1 atm methane partial pressure with high R^2 value of 0.9988. The linear relationship of microsensor 1 on day 2 (Figure 9) had a fairly good linear response to the methane partial pressure (R^2=0.983). Some deviations can be observed, this might result from the electrical interference during the experiments.

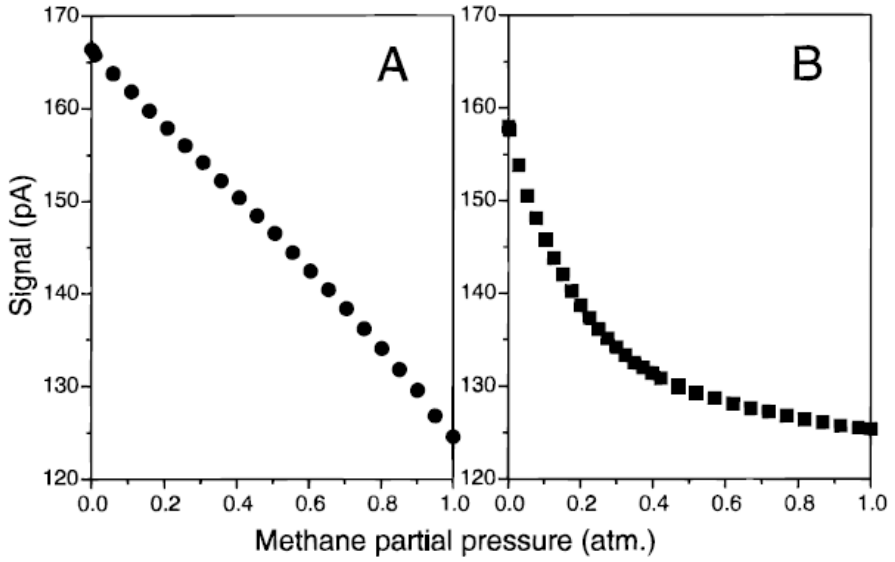

Figure 12 Calibration curves for two methane microbiosensors (A) A linearly responding sensor (B) A nonlinearly responding sensor (Damgaard & Revsbech, 1997)

The calibration curve in Figure 12B had a similar shape as the calibration curves of microsensor 1 and 2 on day 6 and day 5, respectively. Damgaard and Revsbech concluded that sensors which had a longer distance between

the oxygen sensor tip and the gas capillary would have their calibration curves like this. On the contrary, the sensor would exhibit a linear response in the full range of 0-1 atm partial pressure of methane if the distance between them was relatively short.

Some information about the geometry of the two microsensors was shown in Table 2. As it can be seen from the table, although methane microbiosensor 1 had a larger L_{o-g} than methane microsensor 2, it exhibited a linear response on day 2. Additionally, although methane microbiosensor 1 and 2 had different values of L_{o-g}, both microsensors had the no-linear response on day 5 and day 6. And for methane microsensor 1, it could exhibit both types of calibration curves at different times. This suggested L_{o-g} was not playing the major role in determining the shape of the calibration curve in this experiment. On the other hand, bacteria activity could be a major factor that affected the shape of the calibration curve in this experiment. Because when the bacteria were less active, the capacity of the bacteria to consume methane could be exceeded at high concentrations.

Table 2 Information about the geometry of the microsensor 1 and microsensor 2 (unit: μm)

	D_m[a]	D_g[b]	D_o[c]	L_{o-g}[d]	L_{g-m}[e]
Methane microbiosensor 1	190	90	40	55	420
Methane microbiosensor 2	180	90	45	35	100

[a] The tip diameter of media capillary

[b] The tip diameter of gas capillary

[c] The tip diameter of oxygen microsensor

[d] The distance between the tips of oxygen micorsensor and the gas capillary

[e] The distance between the tips of the gas capillary and media capillary

Compared with the methane microbiosensors in Figure 12, methane microbiosensor 1 and 2 both have a relatively long signal range (around 90 pA for methane microsensor 1 and around 800 pA for methane microsensor 2). This showed that methane microbiosensor 1 and 2 had better sensitivity. The results from the calibration demonstrated that the fabrication and calibration process were successful.

4.3 Detection of methane concentrations in an environmental sample

Methane microbiosensors can be used to test methane concentration in aggregated environmental samples. In this study, a sludge sample from an anaerobic digester used for municipal wastewater sludge treatment was chosen. This is because it contained large amounts of methanogens which could generate methane under anaerobic conditions. The sludge was stored in a glass bottle at room temperature and sealed tightly for 2 months. It was then brought in contact with air for 48h before measurements. In this way, a methane concentration gradient could be formed inside the sample.

4.3.1 Sample testing methods

The measurement was performed using methane microbiosensor 1 on day 2 right after the calibration process. Both the calibration and measurement were done at 21℃. The setup for the measurement of the sludge sample was shown

in Figure 13. The methane microbiosensor was fastened onto a micromanipulator which can control the sensor's travel distance. The whole setup was put inside a Faraday cage to reduce the electric interference. A solubility coefficient of 0.034 (Yamamoto, Alcauskas, & Crozier, 1976) corresponding to 24.27 mg/L at 1 atm saturation was used to convert the partial pressure values of methane obtained from calibration and measurements to concentrations. Because oxygen can be a major interference to the signal of methane microbiosensor, the oxygen concentration profile of the sample was also tested by an oxygen microsensor (Unisense, Denmark). The oxygen microsensor was mounted onto the micromanipulator and connected to a picoammeter. The signal at different locations within the sludge sample was recorded.

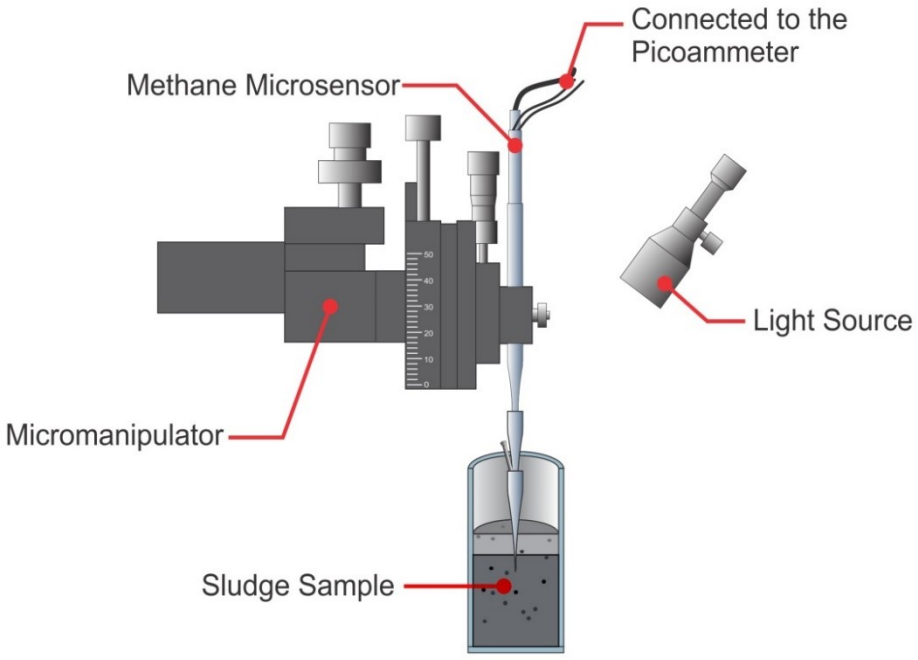

Figure 13 Experimental up for sample testing

4.3.2 Sample testing results

The signal of the methane microbiosensor at each location of the sample was recorded for 100s. The signal stayed relatively stable within 100s. The average of the last 10 stable data at each location was used to generate the methane concentration profile. The error bars represent the standard deviation of the 10 measurements. Because the signal of oxygen microsensor was relatively stable (usually fluctuated within 2 pA), only two reading of the signal were recorded during the measurement. The oxygen profile is

generated with the average value of two readings and the error bars represent the standard deviation of two measurements (Figure 14).

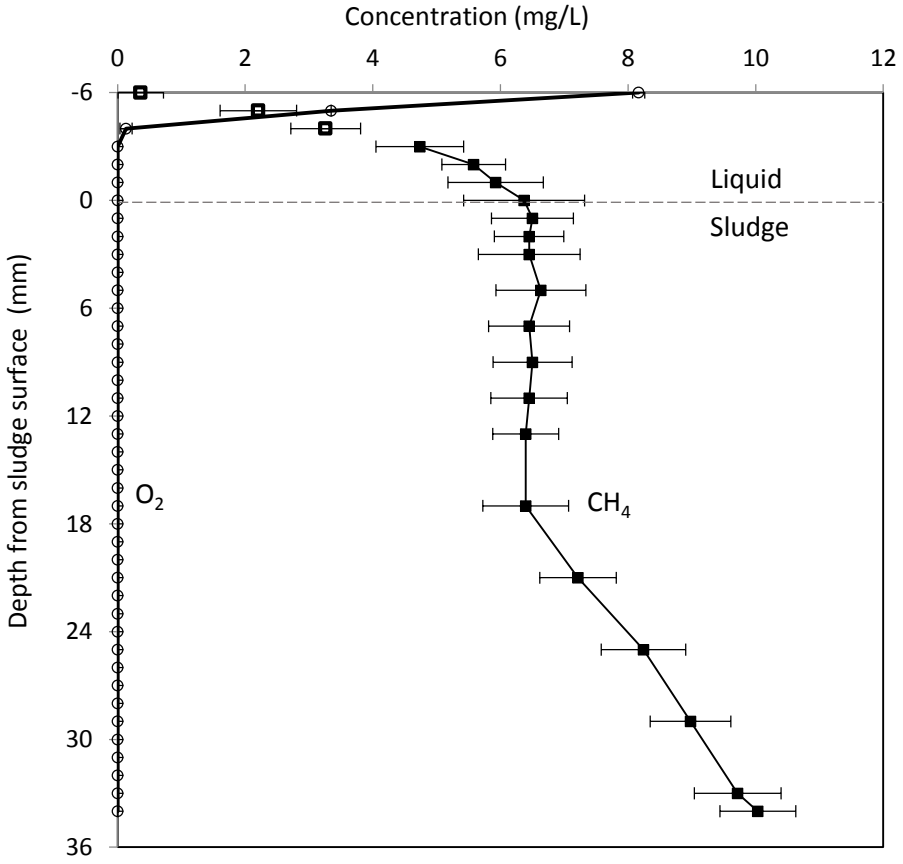

Figure 14 Oxygen and methane concentration profiles

From the concentration profiles in Figure 14, it can be observed that the concentration of oxygen drops from 8.2 mg/L to 0 mg/L, and stays as 0 mg/L from 3 mm depth above the water-sludge interface. Because oxygen can interfere with the signal of the methane microbiosensor, the first 3 data points on the methane concentration profile were not trustworthy.

Methane concentration gradually increased from the surface of the sample to the water-sludge interface (from 0.4 mg/L to 6.4 mg/L). This change is due to the methane in the top layer of the sample was oxidized. From the water-sludge interface to 34mm below the interface, the concentration of methane increased from 6.4 mg/L to 10.0 mg/L. And methanogenesis mainly happened within the range of 17mm to 34mm below the water-sludge interface. Overall, the concentration of methane significantly increased within 4 mm depth in the sample (from 0.4 mg/L to 10.0 mg/L). This is consistent with the fact that the top layer of the sample was exposed to oxygen, and the methane concentration close to the surface is lower than that in deeper parts of the sample. This demonstrated that methane microbiosensor could be applied in the measurements of aggregated environmental samples.

4.4 Limitations of the methane microbiosensor

As it was mentioned in 4.1, oxygen is a major interference gas for the methane microbiosensor. As a result, the applications of methane microbiosensors are only limited to anaerobic conditions.

Due to the decrease of bacteria activity, the linear range of calibration curve can become shorter within one week. To keep the bacteria activity, more maintenance of the sensor should be done after the fabrication. This can be done by exposing the methane microbiosensor to pure methane gas regularly.

Microsensors with larger tip diameters may affect the structure the biofilm during the measurements. Although the tip of the methane microbiosensor is relatively large compared to other microsensors, this microbiosensor can provide otherwise unavailable information in aggregated environmental samples regarding to methanogenesis. The methane microbiosensor can be further improved by making the tip smaller by means of adjusting the geometries of oxygen microsensor, gas capillary and media capillary. Due to the change of the bacterial activity, the calibration curves acquired at different times can be quite different. This will require the sensor to be calibrated each time before the measurements.

5.0 Conclusions and recommendations

Based on the experimental results, the following conclusions can be made:

(1) The methane microbiosensor was successfully fabricated, calibrated and tested in this study, and this fabrication procedure can produce a methane microbiosensor with good performance.

(2) The methane microbiosensor had a tip diameter of around 190 μm and exhibited good linear response to the full range of 0 atm to 1 atm of methane concentration when the bacteria were relatively active.

(3) When the bacteria were less active, the methane microbiosensor could only exhibit linear response at lower concentrations.

(4) Although the tip of the methane microbiosensor is relatively large, the results acquired from the sample measurement have demonstrated the ability of this methane microbiosensor to be used for measurements of methane in aggregated environmental samples.

(5) Bacteria reached its maximum concentration on day 7.

Based on these results, I have the following recommendations for future research:

(1) The tip of the sensor can be made smaller by adjusting the geometries of oxygen microsensor, gas capillary and media capillary.

(2) To keep the bacteria activity, the methane microbiosensor can be exposed to pure methane gas regularly.

(3) Whether or not the change of the cultivation condition (30 ℃ in the incubator at the speed of 300 rpm) will affect the performance of the methane microbiosensor should be further studied.

References

Auschill, T. M., Hein, N., Hellwig, E., Follo, M., Sculean, A., & Arweiler, N. B. (2005). Effect of two antimicrobial agents on early in situ biofilm formation. *Journal of Clinical Periodontology, 32*(2), 147-152.

Bandara, W. M., Satoh, H., Sasakawa, M., Nakahara, Y., Takahashi, M., & Okabe, S. (2011). Removal of residual dissolved methane gas in an upflow anaerobic sludge blanket reactor treating low-strength wastewater at low temperature with degassing membrane. *Water Research, 45*(11), 3533-3540.

Beyenal, H., & Lewandowski, Z. (2005). Modeling mass transport and microbial activity in stratified biofilms. *Chemical Engineering Science, 60*(15), 4337-4348.

Böl, M., Möhle, R. B., Haesner, M., Neu, T. R., Horn, H., & Krull, R. (2009). 3D finite element model of biofilm detachment using real biofilm structures from CLSM data. *Biotechnology and Bioengineering, 103*(1), 177-186.

Characteristic properties of Silicone Rubber Compounds. (2012). Retrieved from http://www.shinetsusilicone-global.com/catalog/pdf/rubber_e.pdf.

Damgaard, L. R., & Revsbech, N. P. (1997). A microscale biosensor for methane containing methanotrophic bacteria and an internal oxygen reservoir. *Analytical Chemistry, 69*(13), 2262-2267.

Denkhaus, E., Meisen, S., Telgheder, U., & Wingender, J. (2007). Chemical and physical methods for characterisation of biofilms. *Microchimica Acta, 158*(1-2), 1-27.

Deutzmann, J. S., Worner, S., & Schink, B. (2011). Activity and diversity of methanotrophic bacteria at methane seeps in eastern lake constance sediments. *Applied and Environmental Microbiology, 77*(8), 2573-2581.

Hawser, S. P., & Douglas, L. J. (1994). Biofilm formation by candida species on the surface of catheter materials in vitro. *Infection and Immunity, 62*(3), 915-921.

Jeroschewski, P., Steuckart, C., & Kühl, M. (1996). An amperometric microsensor for the determination of H2S in aquatic environments. *Analytical Chemistry, 68*(24), 4351-4357.

Kocincova, A. S., Borisov, S. M., Krause, C., & Wolfbeis, O. S. (2007). Fiber-optic microsensors for simultaneous sensing of oxygen and pH, and of oxygen and temperature. *Analytical Chemistry, 79*(22), 8486-8493.

Lackner, S., Terada, A., & Smets, B. F. (2008). Heterotrophic activity compromises autotrophic nitrogen removal in membrane-aerated biofilms: results of a modeling study. *Water research,* 42(4), 1102-1112.

Lazarova, V., & Manem, J. (1995). Biofilm characterization and activity analysis in water and wastewater treatment. *Water Research, 29*(10), 2227-2245.

Lewandowski, Z., & Beyenal, H. (2013). *Fundamentals of biofilm research.* Baco Raton: CRC press.

Liu, H., Tan, S., Sheng, Z., Liu, Y., & Yu, T. (2014). Bacterial community structure and activity of sulfate reducing bacteria in a membrane aerated biofilm analyzed by microsensor and molecular techniques. *Biotechnology and Bioengineering, 111*(11), 2155-2162.

Loupasaki, E., & Diamadopoulos, E. (2013). Attached growth systems for wastewater treatment in small and rural communities: A review. *Journal of Chemical Technology and Biotechnology, 88*(2), 190-204.

Lu, R., & Yu, T. (2002). Fabrication and evaluation of an oxygen microelectrode applicable to environmental engineering and science. *Journal of Environmental Engineering and Science, 1*(3), 225-235.

Metcalf & Eddy. (2014). *Wastewater engineering: Treatment and resource recovery*. New York: McGraw-Hill international ed.

Murrell, J. (2010). The aerobic methane oxidizing bacteria (methanotrophs). In K. N. Timmis (Ed.), *Handbook of hydrocarbon and lipid microbiology* (pp. 1953-1966). New York: Springer.

Okabe, S., Satoh, H., & Watanabe, Y. (1999). In situ analysis of nitrifying biofilms as determined by in situ hybridization and the use of

microelectrodes. *Applied and Environmental Microbiology, 65*(7), 3182-3191.

Park, S., Hanna, L., Taylor, R. T., & Droege, M. W. (1991). Batch cultivation of *Methylosinus trichosporium* OB3b. I: Production of soluble methane monooxygenase. *Biotechnology and Bioengineering, 38*(4), 423-433.

Pompilio, A., Piccolomini, R., Picciani, C., D'Antonio, D., Savini, V., & Di Bonaventura, G. (2008). Factors associated with adherence to and biofilm formation on polystyrene by stenotrophomonas maltophilia: The role of cell surface hydrophobicity and motility. *FEMS Microbiology Letters, 287*(1), 41-47.

Raskin, L., Rittmann, B. E., & Stahl, D. A. (1996). Competition and coexistence of sulfate-reducing and methanogenic populations in anaerobic biofilms. *Applied and Environmental Microbiology, 62*(10), 3847-3857.

Sanz, J. L., & Köchling, T. (2007). Molecular biology techniques used in wastewater treatment: An overview. *Process Biochemistry, 42*(2), 119-133.

Satoh, H., Tsushima, I., Miura, Y., Ito, T., & Okabe, S. (2012). Characterization of microbial community structures and their activities in single anaerobic granules by beta imaging, microsensors and fluorescence in situ hybridization. *Water Science & Technology, 65*(12), 2125-2131.

Satoh, H., Miura, Y., Tsushima, I., & Okabe, S. (2007). Layered structure of bacterial and archaeal communities and their in situ activities in anaerobic granules. *Applied and Environmental Microbiology, 73*(22), 7300-7307.

Schink, B. (1997). Energetics of syntrophic cooperation in methanogenic degradation. Microbiology and Molecular Biology Reviews, 61(2), 262-280.

Scott, D., Brannan, J., & Higgins, I. J. (1981). The effect of growth conditions on intracytoplasmic membranes and methane mono-oxygenase activities in *Methylosinus trichosporium* OB3b. *Microbiology,* 125(1), 63-72.

Sun, J., Hu, S., Sharma, K. R., Ni, B. J., & Yuan, Z. (2014). Stratified microbial structure and activity in sulfide- and methane-producing anaerobic sewer biofilms. *Applied and Environmental Microbiology,* 80(22), 7042-7052.

Takeguchi, M., Miyakawa, K., & Okura, I. (1998). Purification and properties of particulate methane monooxygenase from *Methylosinus trichosporium* OB3b. *Journal of Molecular Catalysis A: Chemical,* 132(2), 145-153.

Tan, S., Yu, T., & Shi, H. (2013). Microsensor determination of multiple microbial processes in an oxygen-based membrane aerated biofilm. *Water Science and Technology,* 69(5), 909-914.

Wolf, G., Crespo, J. G., & Reis, M. A. (2002). Optical and spectroscopic methods for biofilm examination and monitoring. *Reviews in Environmental Science and Biotechnology,* 1(3), 227-251.

Xavier, J., White, D., & Almeida, J. (2003). Automated biofilm morphology quantification from confocal laser scanning microscopy imaging. *Water Science & Technology,* 47(5), 31-37.

Xin, J. Y., Cui, J. R., Hu, X. X., Li, S., Xia, C., Zhu, L., & Wang, Y. (2002) Particulate methane monooxygenase from *Methylosinus trichosporium* is a copper-containing enzyme. *Biochem Biophys Res Commu,* 295(1), 182–186.

Yamamoto, S., Alcauskas, J. B., & Crozier, T. E. (1976). Solubility of methane in distilled water and seawater. *Journal of Chemical and Engineering Data, 21*(1), 78-80.

Yoshida, A., & Kuramitsu, H. K. (2002). Multiple streptococcus mutans genes are involved in biofilm formation. *Applied and Environmental Microbiology, 68*(12), 6283-6291.

Yu, T., & Bishop, P. L. (1998). Stratification of microbial metabolic processes and redox potential change in an aerobic biofilm studied using microelectrodes. *Water Science and Technology, 37*(4), 195-198.

Yu, T., & Bishop, P. L. (2001). Stratification and oxidation–reduction potential change in an aerobic and sulfate-reducing biofilm studied using microelectrodes. *Water Environment Research, 73*(3), 368-373.

Zinder, S. H. (1993). Physiological ecology of methanogens. In J. G. Ferry (Ed.), *Methanogenesis* (pp. 128-206). New York: Springer.

Appendices

Appendix A: Raw Data

Appendix A: Raw Data

Table A-1 Summary of experimental data of calibration for methane microbiosensor 1 on day 2

Partial Pressure (atm.)	Signal Average(pA)
0.000	202
0.031	200
0.063	201
0.094	198
0.125	197
0.156	186
0.188	180
0.219	176
0.250	174
0.281	172
0.313	167
0.344	168
0.375	165
0.406	161
0.438	159
0.469	157
0.500	153
0.531	150
0.563	146
0.594	144
0.625	143
0.656	140
0.750	133
0.813	129
0.875	124
0.938	118
1.000	114

Table A-2 Summary of experimental data of calibration for methane microbiosensor 1 on day 6

Partial Pressure (atm.)	Signal Average(pA)
0.000	337
0.025	329
0.050	323
0.075	318
0.100	313
0.125	309
0.150	307
0.175	305
0.200	302
0.225	302
0.250	301
0.275	299
0.300	299
0.325	298
0.350	297
0.375	297
0.400	296
0.425	295
0.450	296
0.475	295
0.500	296
0.550	295
0.600	295
0.700	295
0.800	296
0.900	296
1.000	295

Table A-3 Summary of experimental data of calibration for methane microbiosensor 2 on day 5

Partial Pressure (atm.)	Signal Average(pA)
0.000	1601
0.059	1534
0.118	1459
0.176	1381
0.235	1226
0.294	1045
0.353	952
0.412	927
0.471	885
0.529	866
0.588	861
0.647	851
0.706	848
0.765	847
0.824	846
0.882	840
0.941	837
1.000	831

Table A-4 Summary of experimental data of sample testing for methane concentration

Depth(mm)	Signal Average(pA)
-6	200
-5	193
-4	189
-3	183
-2	180
-1	178
0	177
1	176
2	176
3	176
5	176
7	176
9	176
11	176
13	177
17	177
21	174
25	170
29	167
33	164
34	163

Table A-5 Summary of experimental data of sample testing for oxygen concentration

Depth(mm)	Signal Average(pA)
-6	64
-5	28
-4	4
-3	3
-2	3
-1	3
0	3
1	3
2	3
3	3
4	3
5	3
6	3
7	3
8	3
9	3
10	3
11	3
12	3
13	3
14	3
15	3
16	3
17	3
18	3
19	3
20	3
21	3
22	3
23	3
24	3
25	3
26	3
27	3
28	3
29	3
30	3
31	3
32	3
33	3
34	3

Table A-6 Summary of experimental data of OD of bacterial

Time (Day)	OD		
	Sample 1	Sample 2	Sample 3
0	0.019	0.024	0.019
1	0.016	0.024	0.024
2	0.028	0.036	0.031
3	0.027	0.036	0.036
4	0.021	0.029	0.035
5	0.026	0.031	0.032
6	0.024	0.036	0.031
7	0.032	0.04	0.043
8	0.03	0.039	0.039
9	0.031	0.036	0.04
10	0.027	0.034	0.034